Published in final edited form as:
J Immunol. 2014 March 1; 192(5): 2405–2417. doi:10.4049/jimmunol.1302752.

G-CSF Drives a Post Traumatic Immune Program that Protects the Host from Infection[1]

Jason C. Gardner[†], **John G. Noel**[§], **Nikolaos M. Nikolaidis**[†], **Rebekah Karns**[¶], **Bruce J. Aronow**[¶], **Cora K. Ogle**[‡,§], and **Francis X. McCormack**[†]

[†]Division of Pulmonary, Critical Care and Sleep Medicine, University of Cincinnati

[‡]Division of Research, Department of Surgery, University of Cincinnati

[§]Department of Research, Shriners Hospitals for Children, Cincinnati, OH

[¶]Cincinnati Children's Hospital Medical Center

Abstract

Traumatic injury is generally considered to have a suppressive effect on the immune system, resulting in increased susceptibility to infection. Paradoxically, we found that thermal injury to the skin induced a robust time-dependent protection of mice from a lethal *Klebsiella pneumoniae* pulmonary challenge. The protective response was neutrophil dependent and temporally associated with a systemic increase in neutrophils resulting from a reprioritization of hematopoiesis toward myeloid lineages. A prominent and specific activation of STAT3 in the bone marrow preceded the myeloid shift in that compartment, in association with durable increases in STAT3 activating serum cytokines G-CSF and IL-6. Neutralization of the post burn rise in serum G-CSF largely blocked STAT3 activation in marrow cells, reversing the hematopoietic changes and systemic neutrophilia. Daily administration of recombinant G-CSF was sufficient to recapitulate the changes induced by injury including hematopoietic reprioritization and protection from pulmonary challenge with *K. pneumoniae*. Analysis of posttraumatic gene expression patterns in humans reveals that they are also consistent with a role for G-CSF as a switch that activates innate immune responses and suppresses adaptive immune responses. Our findings suggest that the G-CSF STAT3 axis constitutes a key protective mechanism induced by injury to reduce the risk of post-traumatic infection.

Introduction

The human response to traumatic injury has recently been described as a 'genomic storm', in which the whole blood leukocyte transcriptome is reshaped by a concomitant induction of innate immunity genes and suppression of adaptive immunity genes (1). These gene expression changes occur in both survivors and nonsurvivors, but the poorest outcomes are associated with an excessive magnitude and duration of the molecular response. Trauma, burn injury, and to some degree LPS exposure all result in a similar pattern of gene expression. The conserved molecular response to different stressors is thought to be driven by channeling of signals through shared pathways responsive to TLR4 activation, pathogen-

[1]This work was supported by Shriners of North America Grant #86300 and #85120 The project described was supported by the National Center for Research Resources and the National Center for Advancing Translational Sciences, National Institutes of Health, through Grant 8 UL1 TR000077-05. The content is solely the responsibility of the authors and does not necessarily represent the official views of the NIH.

Address correspondence to: Jason C. Gardner, Ph.D. Dept. of Pulmonary, Critical Care and Sleep Medicine. University of Cincinnati Medical Center, PO Box 670564, Cincinnati, OH 45267-0564, Tel 513-558-4831, Fax 314-454-5917, gardnejr@ucmail.uc.edu.

associated molecular patterns, damage-associated molecular patterns, or alarmins, however, no specific factors have been implicated in the induction of the ‘genomic storm’.

On a functional level, animal studies indicate that injury primes an enhanced innate immune reactivity resulting in excess production of soluble inflammatory mediators including TNFα, IL-6, and IL-1β (2, 3) and heightened TLR-2 and TLR-4 reactivity (2, 4, 5). In trauma patients, circulating neutrophils are quantitatively increased, display a higher level of activation as measured by CD11b surface staining, and produce an increased oxidative burst upon stimulation (6). Triggering of deleterious inflammatory cascades by innate immune responses such as these is widely considered to contribute to high rates of lethal multiple organ failure in trauma patients (7). However, some animal models suggest that injury-induced augmentation of innate immunity may play a beneficial role in preventing infection. Several reports indicate that within a week of burn injury, mice display a heightened level of resistance to infection following intraperitoneal challenge with *Escherichia coli* or *Pseudomonas aeruginosa* (8, 9) or subcutaneous challenge with *P. aeruginosa* (10-12). In studies that explored the mechanism of the protective phenomenon, resistance to infection developed with time after injury and was associated with increased numbers of functionally enhanced phagocytes. Our group recently reported that mice that were protected from subcutaneous infection eight days after burn injury also exhibited increased mortality when challenged with LPS (10). This effect was abrogated following global depletion of myeloid cells with gemcitabine, suggesting that inflammatory tone and burn-induced resistance to infection are linked.

In contrast to the enhanced innate immune reactivity, several lines of evidence demonstrate that adaptive immune functions in burn injured animals and humans are suppressed. These include prolonged skin-homograft survival, reductions in delayed type hypersensitivity reactions, and impaired lymphocyte responses (13-15). Early after burn injury and for up to several days thereafter, quantitative reductions in T cell populations occur due to apoptosis (16, 17) and lymphocyte proliferative responses are impaired (18). Production of IL-2, IFN-γ, and IL-12 are reported to be preferentially suppressed following burn injury (19, 20), while production of IL-4 and IL-10 are increased (21), consistent with a Th-1 to Th-2 phenotypic switch. Th1 suppressing CD4+CD25+ T regulatory cells are suspected to play a role in the suppression of Th1 responses seen in injured humans and mice. (22, 23). Additionally, our group has previously noted that global depletion of myeloid cells with gemcitabine restores T-lymphocyte proliferative function in burn injured mice (10), suggesting that myeloid cells also play a role in the suppression of adaptive immune function following injury.

Traumatic injury also results in profound changes in hematopoiesis in mice and humans, best characterized as a hematopoietic reprioritization in which myeloid cells expand in the marrow while other lineages are reduced (24, 25). The reprioritization of the marrow away from red cell production occurs despite high levels of circulating erythropoietin (EPO) in trauma patients and in burn-injured mice EPO administration does not restore normal reticulocytosis. Human burn victims are also refractory to treatment with EPO (26). Marrow reprioritization is thought to contribute to the EPO resistant anemia of critical illness, which accounts for more than 50% of the transfusion requirements in burn patients (27).

Although the described injury-induced changes in innate and adaptive immune function as well as the alteration of marrow priorities have been a prominent focus of trauma research over several decades, no study has systematically linked these changes to a specific factor or factors induced by injury. In this study, we demonstrate that thermal injury of the skin in mice results in a paradoxical protection against a lethal Klebsiella pneumoniae pulmonary infection, associated with a myeloid specific activation of STAT3 in the marrow,

hematopoietic reprioritization, and a systemic expansion of functionally enhanced neutrophils. We provide evidence that these processes in mice are driven by G-CSF, and that remarkably congruent human gene expression profiles for G-CSF administration and trauma are consistent with a central role for G-CSF as a regulator of the 'genomic storm', driving divergent innate and adaptive immune responses following traumatic injury.

Materials and Methods

Mouse injury model

All procedures were approved by the University of Cincinnati Institutional Animal Care and Use Committee. Non-Swiss Albino Outbred Mice Hsd:NSA™(CF-1®) were purchased from Harlan Laboratories (Indianapolis, IN). The burn procedure employed results in a full thickness injury, as previously described (11, 28). Briefly, mice were anesthetized with isoflurane and covered with a flame-resistant template exposing a dorsal skin section equivalent to 15% of total body surface area. The target area was saturated with 0.5ml of absolute ethanol, and either ignited for 10 seconds or allowed to evaporate without ignition. Immediately following burn or sham procedure, mice received 0.5ml of saline for volume resuscitation via the intraperitoneal (i.p.) route.

Infection procedure and quantitative culture

Klebsiella pneumoniae KP2 2-70, a virulent and highly encapsulated Gram-negative bacterial strain (29, 30), was grown overnight in brain heart infusion (BHI) broth. The following morning bacteria were washed in Dulbecco's phosphate buffered saline (DPBS) without metals, and administered at 4×10^4 cfu/50 μl by the intranasal route to isoflurane-anesthetized mice. For quantitative culture, the lung and spleen were removed from infected mice, homogenized in DPBS without metals, and plated on trypticase soy agar (TSA). Colony forming units were quantified after overnight incubation at 37°C.

Isolation of whole lung and blood cells

Whole lung tissue cells were isolated in a two-step protocol using a gentleMACS Dissociator according to manufacturer's instructions (Miltenyi Biotec, Auburn, CA). Dissociation buffer was comprised of 4ml of DPBS, 150U/ml Type IV collagenase (Worthington Biochemical. cat#LS004188), and 50U/ml Dnase (Worthington biochemical #LS002139). Cell suspensions were filtered through 70um filters and washed with DPBS. Leukocytes were isolated by Lympholyte-M separation (Cedarlane Laboratories, Ontario, Canada). Blood was collected by cardiac puncture and stored in EDTA coated tubes prior to analysis using the Hemavet® 950 system (Drew Scientific, Waterbury, CT).

Quantitative depletion of neutrophils

Neutrophils were depleted with 200μg of anti-Ly6G (clone 1A8) (BioXcell, West Lebanon, NH), delivered i.p. in a 100ul volume of saline one day prior to infection and again at the time of infection. Rat IgG2a clone 2A3 (BioXcell, West Lebanon, NH) was used as an isotype control, delivered at the same dose and by the same route and schedule as the neutrophil depleting antibody.

BAL cell collection and oxidative burst

Bronchial alveolar lavage (BAL) was performed by 3 cycles of infusion and aspiration using 0.7ml of HBSS, repeated 3 times. Recovery was routinely 80% of instilled volume or greater. Harvested BAL cells were collected by centrifugation at 500×g for 5 minutes, washed, counted, and resuspended in FACS buffer prior to staining with antibodies for flow cytometry. For analysis of oxidative burst, BAL cells were collected 4 hours after intranasal

challenge with *K. pneumoniae* at 4×10^4 cfu/mouse. Cells were incubated in HBSS + 5μM DHR123 (Invitrogen, Cat# D-23806) at 37°C for 10 minutes, stimulated with 1uM phorbol 12-myristate 13-acetate (PMA, Sigma-Aldrich, Cat# P1585) for 30 minutes, placed on ice and stained for FACS analysis. Neutrophils were identified by the staining pattern: CD45+ CD11b+ Ly6G+ F4/80−.

Serum and bronchial alveolar lavage fluid cytokine determinations

For isolation of serum, whole blood was collected by cardiac puncture, allowed to clot on ice and centrifuged in BD Microtainer® serum separator tubes. BAL fluid for cytokine quantitation was from the first cycle of infusion and aspiration described in BAL method. Serum and BAL fluid were frozen at −70°C until analysis using Milliplex MAP Kits (Millipore, Billerica, MA) according to manufacturer's protocol. Plates were read on the Bio-Plex (Bio-Rad, Hercules, CA) and concentrations were calculated using recombinant protein standards. Cytokine analysis was performed by the Research Flow Cytometry Core at Cincinnati Children's Hospital Medical Center.

Bone marrow cell harvest and phosflow cytometry

Bone marrow isolation was performed by flushing the femurs of mice with 1.5 ml of HBSS, then filtering the eluate through 70 μm filters. Following resuspension in media or FACS buffer (DPBS with 1% BSA and 0.1% sodium azide, PH 7.3), phosphoproteins were measured by the method of Nolan et al (31), with minor modifications allowing for rapid isolation and paraformaldehyde fixation. Briefly, bone marrow cells were isolated as above and immediately fixed at a final concentration of 1.6% paraformaldehyde in DPBS. After incubation for 10 min at RT, the reaction was stopped by dilution with ice cold FACS buffer and all subsequent processing was conducted in the cold. The samples were filtered through a 70 μm filter, pelleted at 400×g for 10 minutes, and then resuspended to a volume of 0.2 ml. Two ml of 100% ice cold methanol were added to the pellet with vortexing. The samples were kept at −20°C until staining, then washed with FACS buffer and stained with antibodies to surface markers to phenotype the cells as well as with antibodies to characterize the phosphorylation state of intracellular signaling molecules. In the initial screening assay, Fluorescence Minus One (FMO) controls, were used to set backgrounds and control for interference among fluorescence channels (32). Cells were interrogated for phosphorylation of the following proteins (residues): PE-AKT(pT308), PE- p38(pY182/pT180), AF647-ERK(pY202/pT204), AF-647STAT3(pY705), PE- STAT5(pY694), and AF647STAT1(pY701) (BD Biosciences, San Jose, CA). For the time course of pSTAT3 background staining was evaluated with labeled pSTAT3 antibody in the presence of a ten-fold excess of unlabeled pSTAT3 antibody. In these experiments, identification of bone marrow cell subtypes was performed as described in the flow cytometry methods section.

Flow cytometry and identification of cell subtypes

Cells isolated from lung or bone marrow were resuspended in FACS buffer (DPBS, 0.1% sodium azide, and 1% bovine serum albumin). Nonspecific binding was blocked by using 2μl Fc Block (BD Biosciences) and 5μl rat serum per 100 μl cell staining volume. Bone marrow cells were stained with fluorescently labeled antibodies to CD45(leukocytes), CD45R(B cells) , TER119(red cells) , CD117(progenitors), CD11b(myeloid cells) and CD34(myeloid progenitors) (Biolegend or Ebiosciences, San Diego, Ca). Antibodies to LY6G and LY6C were used to identify CD11b+ LY6G+ neutrophils and CD11b+ LY6C+ monocytes (BD Biosciences, San Jose, Ca.). All antibodies were directly conjugated with FITC, PE, Percp CY 5.5, APC, E450, or Brilliant Violet 421 dyes. Lung leukocyte composition was determined by FACS analysis of CD45+ cells. Markers used to differentiate leukocyte subsets were as follows; Tcells(CD3+), Bcells(CD45R+), alveolar

macrophages (CD11c+, F4/80+, CD11b−/dim), dendritic cells (CD11c+,CD11b+) , PMN (CD11c−, F4/80−, CD11b+, Ly6G+), macrophage-monocytes (also known as resident monocytes) (CD11c−, F4/80+, CD11b+, Ly6C−/+), inflammatory monocytes (CD11c−, F4/80+, CD11b+, Ly6C++). FMO controls were used and fluorescence compensation was performed using singly labeled cells, BD Comp Beads or BD Comp Beads Plus (BD Biosciences). Samples were run on a FACS LSRII-a tabletop flow cytometer using four lasers (325, 405, 488, 633 nm), and capable of detecting 13 parameters per cell/particle (Becton Dickenson). Data was analyzed using FCS Express Flow Cytometry Software.

In vivo neutralization of G-CSF

Mice were treated i.p. with 10μg of anti-G-CSF (R&D Systems, Cat# MAB414) or isotype control IgG (R&D Systems, Cat# MAB005) in a 100μl volume of saline 12 hours prior to injury. Antibody dosing was repeated at the time of injury and daily on days 1 through 6 post injury for a total of 8 doses. Bone marrow cells and blood were harvested on day 7 post injury.

Recombinant G-CSF treatment

Mice were injected i.p. twice daily with 7.5 μg/kg carrier free murine G-CSF (R&D Systems) in a volume of 100μl PBS or with PBS alone for 6 consecutive days. On day 7, mice were sacrificed for determination of bone marrow composition by flow cytometry or infected with *K. pneumoniae* i.n. at 4×10^4 cfu/mouse. The vital status of infected mice was followed for 2 weeks.

Comparison of whole blood leukocyte gene expression profiles of G-CSF treated humans and trauma victims

Gene Expression Omnibus experiments GSE7400 (Granulocyte colony-stimulating factor mobilized leukocytes) and GSE36809 (A genomic storm in critically injured humans) were analyzed in GeneSpring 12.5, using RMA normalization and base-lining each experiment's data to the median of controls. In both data sets we performed analysis of variance to generate gene lists with differential regulation between controls and post-trauma (each time point was assessed) and post-G-CSF administration with p<=0.05. Among the significant genes, those with a fold change of >=2.0 were considered to have differential expression levels. Based on the list of genes with p<=0.05 and fold change >=2 generated in the Genomic Storm experiment, fold change correlation between trauma and G-CSF effect was assessed through Pearson's correlation. Trauma and G-CSF gene lists were intersected to determine overlapping expression patterns; genes differentially regulated in both experiments were submitted to ToppGene (toppgene.cchmc.org) for ontological analysis.

Statistics

Statistical analysis was performed using GraphPad Prism 5. The Wilcoxon test was used to determine differences in survival curves. The Mann-Whitney test was used to compare bacterial counts in burn vs. sham groups. The Student's T-test was used for burn vs. sham comparisons at specific time points, and ANOVA was used when multiple groups were compared.

Results

Thermal injury of the skin induces a time-dependent reduction in *K. pneumoniae* induced mortality, associated with enhanced pulmonary bacterial clearance

To determine if mice develop resistance to a lethal pulmonary infection with time following thermal injury, as has been reported in models of post burn skin and intraperitoneal

infection, we challenged mice i.n. with 4×10^4 cfu of *K. pneumoniae* at 2 hours or 7 days after administering a sham injury or 15% total body surface area burn. Vital status was monitored over a 2 week period following infection. The survival curves of the burn and sham groups were very similar when the infectious challenge was delivered 2 hours after injury, with about 50% of mice dying by day 6 (fig. 1A), but the mortality of the groups diverged substantially when mice were challenged at 7 days post injury (fig. 1B). The burned animals had a marked survival advantage compared to their sham counterparts at that late time point ($p<.01$ burn vs. sham). Quantitative culture of homogenized lung and spleen tissues was performed at 24 and 48 hours post infection in mice challenged at day 7 post injury (fig.1C&D). At 24 hours, the burden of organisms in the lungs of the burned animals was very similar to that of the original inoculum, and fell two logs by 48 hours, consistent with progressive clearance of the organism from the lung. In the sham group, the burden of organisms at 24 hours was about one log higher than that of the original inoculum and that of the burn group, and did not fall by 48 hours, indicating failure of clearance. Splenic CFU were also quantified as an index for systemic bacterial dissemination. No bacterial colonies were detected in homogenized splenic tissue at 24 hours, but by 48 hours CFUs were two logs greater in the sham group than the burn group.

Thermal injury induces a neutrophilic response in lung and blood after 7 days

To evaluate the role of inflammation in the time-dependent, burn-induced protection from infection we examined the leukocyte composition of lung tissue and peripheral blood harvested from uninfected, day 7 post burn and sham injured mice. FACS analysis of whole lung tissue from burned mice revealed a significant increase in lung-associated neutrophils, an increase in inflammatory monocytes and a reduction in B cells (fig.2A), relative to sham injured controls. Proportions of lung tissue associated T cells, alveolar macrophages, dendritic cells, and monocytes were not different between the groups. Quantitation of peripheral blood leukocytes revealed an increase in circulating neutrophils in the burn group compared to the sham group, but no differences in total white blood cell counts, lymphocytes, or monocytes were detected in circulating cells (fig.2B). The systemic neutrophilic response was accompanied by a reduction in red blood cell numbers, as well as in hemoglobin, and hematocrit (fig.2C).

The protection from pulmonary infection induced by thermal injury is neutrophil dependent

The role of the neutrophilic response in thermal injury induced resistance to infection was assessed by quantitative depletion of neutrophils in burn and sham injured mice prior to infectious challenge. The neutrophil depleting antibody, anti-Ly6G (clone 1A8), or an isotype control antibody was administered i.p. on day 6 post injury and at the time of infection on day 7 post injury. The protection from pulmonary infection induced by injury was apparent in isotype treated mice, with a substantial mortality reduction in the burn-injured group compared to sham controls ($p<.01$ burn isotype vs. sham isotype). The survival curves for the anti-Ly6G sham and burn groups were overlapping with each other and with the isotype-antibody treated sham control, indicating that protection afforded by burn injury was completely reversed by neutrophil depletion (fig.3).

Assessment of airspace neutrophil recruitment, oxidative burst, and BAL cytokine levels indicates neutrophils from thermally injured mice are primed for an enhanced oxidative response

To quantify neutrophil recruitment, 7 day post burn or sham injured mice were challenged with 4×10^4 *K. pneumoniae* and BAL cells were collected for neutrophil quantitation by FACS at 0, 4, and 24 hours post challenge (fig.4A). Prior to infection, F4/80− Ly6G+ cells

(neutrophils) comprised less than 1% of airway cells. Upon administration of the bacterial inoculum, a similar increase in neutrophils was seen in sham and burn injured mice, reaching approximately 10% of airway cells at 4 hours post challenge. After 24 hours of infection, a trend towards greater increases in neutrophils in the sham injured mice appeared to be developing, however statistically significant differences between the groups were not seen at any time point.

To assess the effect of thermal injury on the functional state of neutrophils recruited to the airspace early after infection, we challenged 7 day post burn or sham injured mice i.n. with 4×10^4 *K. pneumoniae.* Four hours later, BAL cells were isolated and stimulated with PMA, then subjected to FACS analysis to quantify the oxidation-driven conversion of DHR123 to fluorescent R123, as well as CD11b surface expression; measures of oxidative burst and degranulation respectively (33). BAL neutrophils from burn injured mice responded to PMA stimulation with a more robust oxidative response and greater degree of degranulation (fig. 4B) than did those from sham mice.

To evaluate potential differences in airspace inflammatory tone between sham and burn injured mice we quantified soluble inflammatory mediators present in BAL fluid collected 0, 4, and 24 hours post infection of mice challenged with K. pneumonia on day 7 post thermal injury. Prior to infection, all analytes tested were below the detectable limit of our assay (data not shown). At 4 hours post infection, the time at which cells were collected for functional assays, levels of G-CSF, IL-6, KC, MIP-2, and TNFα were all found to be elevated, to levels that were similar between burn and sham treated groups (fig.4C). After 24 hours of infection there was a trend towards increased levels of several inflammatory cytokines and chemokines in sham injured mice compared to the burned animals, although these between group differences did not reach statistical significance (fig.4D).

Time-dependent, injury-induced protection from pneumonia is temporally associated with hematopoietic reprioritization

Experiments were performed to test the hypothesis that post burn alterations in hematopoiesis may explain time-dependent quantitative and functional neutrophil responses, and resistance to infection. In the marrow, we found a myeloid expansion (CD11b+ cell percentage) in the burn group compared to sham controls that was evident by 3 days post injury and was further increased by day 7 post injury (fig.5A), largely attributable to a rise in neutrophils and monocyte numbers (fig.5B). Concurrent with the increase in myeloid cells, there was a reduction in B cells and red blood cell lineages. Total bone marrow cell counts were not significantly different between burn and sham injured groups (fig.S1A), indicating that an expansion of myeloid populations was counterbalanced by a reduction in other lineages. This reprioritization of the marrow was consistent with post injury day 7 changes in cellular compositions of blood and whole lung tissue, including systemic increases in neutrophils and inflammatory monocytes, and reductions in circulating red blood cells and B cells in whole lung tissue. To assess differences in progenitor populations, we isolated bone marrow from 7 day post sham and burn injured mice and determined the proportion of CD117+CD34+ which are primarily composed of myeloid progenitors (80-90%) relative to CD117+CD34− megakaryocyte/erythrocyte progenitors. We found that changes in the progenitor populations mirrored those of the mature cells in the marrow and the circulation, exhibiting a shift toward myeloid lineages (fig.5C).

Cytokine response and bone marrow signaling suggest STAT3 activation is a primary driver of thermal injury induced hematopoietic reprioritization

Experiments were performed to explore the factors driving marrow reprioritization and resistance to pulmonary infection following thermal injury. Serum was collected prior to

insult and at 6hrs, 1 day, 3 days, and 7 days after burn or sham treatment, and samples were screened for 42 cytokines by multiplex analysis. Serum concentrations of G-CSF, IL-6, and KC peaked sharply within one day in the burn group relative to the sham group, with persistent elevation of G-CSF and IL-6 (albeit at declining levels) for 7 days (fig. 6A). Remarkably, there were no consistent elevations in other serum cytokines in the multiplex panel. We used phosphlow to detect injury activated phosphorylation of key nodes in the Akt, STAT, MAPK and ERK signaling pathways in mature (CD11b+) and progenitor (CD117+) bone marrow cells. Although constitutive activation of several pathways was suggested in our initial screen of bone marrow cells from burn and sham injured mice, STAT3 was the only pathway that was found to be differentially activated in response to burn injury, in both progenitors and mature myeloid cells (fig.6B).

Bone marrow STAT3 activation is durable and specific to myeloid cells and myeloid progenitors following burn injury

We next investigated the durability and cellular specificity of STAT3 activation. Bone marrow cells were harvested for phosphlow prior to insult and at 6hrs, 1 day, 3 days, and 7 days post burn or sham treatment. The STAT3 response was interrogated over time by gating on (CD11b+Ly6G+) neutrophils, (CD11b+Ly6G−) monocytes, (CD11b-Ly6G−) non-myeloid cells, (CD117+CD34−) megakaryocyte erythrocyte progenitors, and (CD117+CD34+) myeloid progenitors (fig.7A). Histograms from representative bone marrow samples isolated at 1 day post burn or sham demonstrate that STAT3 activation is specifically increased in neutrophils, monocytes, and myeloid progenitors following burn injury, as activation of this signaling intermediate was not seen in non-myeloid bone marrow cells or in megakaryocyte erythrocyte progenitors (fig.7B). STAT3 activation in the mature and progenitor myeloid cells from burned animals was sustained above baseline for up to a week (fig.7C). The patterns of increased STAT3 activation in the burned animals and elevation of serum G-CSF and IL-6 were strikingly similar, suggesting a possible causal role for the cytokines in driving STAT3 signaling in the marrow (34, 35). These findings led us to postulate that G-CSF, IL-6 and STAT3 constitute an axis that is responsible for the post burn hematopoietic reprioritization and protection from pulmonary infection.

Neutralization of post burn serum G-CSF prevents myeloid specific STAT3 activation, bone marrow reprioritization, and neutrophilia

We employed an *in vivo* neutralization strategy to determine if G-CSF is necessary for the post burn bone marrow reprioritization and neutrophilia. Anti-G-CSF antibody blocked nearly 80% of the STAT3 activation induced by thermal injury in CD117+CD34+ bone marrow progenitors at 6 hours post burn (fig.8A&B). Similar reductions in STAT3 activation were seen in bone marrow neutrophils and monocytes upon G-CSF neutralization (data not shown).

Mice were treated with anti-G-CSF or isotype antibody before and at the time of injury, then for 6 days following injury. On day 7 post burn or sham treatment, bone marrow and blood were obtained for analysis. Neutralization of G-CSF prevented hematopoietic reprioritization following burn injury (fig.8C). Thermal injury induced reductions in B cell and red cell numbers in the marrow were significantly blocked by neutralizing serum G-CSF post burn, as were burn induced increases in marrow neutrophils and monocytes. These changes represented a compositional shift of the bone marrow as total cell counts were not found to be different (fig.S1B). Neutralization of G-CSF also prevented the neutrophilia at one week post burn injury (fig.8D). Although administration of anti-G-CSF blocked the post burn reduction of red cells in the bone marrow, the peripheral reduction in red cells shown in figure 2C was still evident in these mice (data not shown).

Recombinant G-CSF is sufficient to recapitulate hematopoietic alterations induced by injury and protection from a lethal K. pneumoniae infection

Experiments were performed to test the hypothesis that G-CSF is sufficient for bone marrow reprioritization and protection from a lethal *K. pneumoniae* pulmonary infection, as is seen following burn injury. We administered recombinant G-CSF i.p. in 2 daily doses of 7.5 μg/kg for a total daily dose of 15 μg/kg. A control group of mice was given an equal volume of saline on the same schedule. After six consecutive days of treatment, bone marrow was harvested on day 7 to assess cellularity. Total bone marrow cellularity was not different in G-CSF vs. PBS treated mice (fig.S1C) and alterations reflected a change in bone marrow composition with an increase in myeloid cells at the expense of other lineages (fig.9A). Similar to the marrow changes seen in post burn day 7 mice, neutrophils and monocytes were increased, while B cells and red cells were decreased as a percentage of bone marrow cells. Daily G-CSF treatment for six days was also found to provide a survival advantage (p=.054 G-CSF vs. PBS) in mice that were given a lethal *K. pneumoniae* pulmonary inoculum 24 hours after the final G-CSF dose (fig.9B).

In humans, recombinant G-CSF largely reproduces the ‘genomic storm’ that follows traumatic injury

Having determined that G-CSF plays an important role in the murine response to traumatic burn injury and infection, we postulated that it may be a critical factor in the human response to trauma as well, based on analogous biological function and receptor binding cross reactivity in mice and humans (36). To explore the role of G-CSF in the human response to trauma we compared the whole blood leukocyte transcriptional response that follows traumatic injury (1) to the response that is seen in humans treated with G-CSF for the mobilization of hematopoietic stem cells (37). In this comparison, we found that of the genes with expression changes of 2 fold or more following trauma, 92% had the same direction of effect following consecutive doses of G-CSF (fig.10A). Correlation analysis of fold changes following trauma and G-CSF, using genes with at least a 2 fold change following trauma, indicated high correlation (R=0.65) of expression patterns between trauma victims and those treated with G-CSF (fig.10B). Most importantly, many of the genes upregulated in response to trauma and G-CSF treatment were associated with innate immunity, while genes that were commonly downregulated in response to trauma and G-CSF treated are associated with adaptive immunity (fig.10C).

Discussion

We have found that thermal injury of the skin induces a robust protection against a lethal *K. pneumoniae* pulmonary challenge delivered to mice 7 days later, while no protection is afforded by injury if the infection is delivered 2 hours after the initial trauma. Our data demonstrate that the time-dependent resistance to infection is associated with enhanced ability to clear bacteria from the lung and reduced systemic dissemination. We found that the protective response coincided with a systemic increase in neutrophils and was neutrophil dependent.

We determined neutrophil recruitment to the airspace was not increased in burn injured mice following infection despite the systemic increase in neutrophils prior to infection. BAL neutrophils isolated from 7 day post burn injured mice, early after *K. pneumoniae* challenge, were found to respond to stimulus with a greater respiratory burst and degranulation response, consistent with enhanced antimicrobial capacity. BAL cytokine and chemokine levels in burn-injured mice were not found to be different following infection; indeed, there was a trend toward lower levels of BAL neutrophils and inflammatory mediators in that group, most likely reflecting the lower bacterial burden in burn injured mice. Together, these

results suggest the posttraumatic neutrophil dependent protection from infection is more likely attributable to cellular antimicrobial function enhancement than to quantitative increases in neutrophils.

An unbiased screen of post burn serum cytokines identified a durable and highly specific increase in the STAT3 activating cytokines G-CSF and IL-6, which preceded myeloid expansion in the bone marrow and a systemic increase in neutrophils. Neutralization experiments indicate that G-CSF is the primary activator of STAT3 in mature myeloid cells and myeloid progenitors in the marrow following thermal injury. In addition, our data suggest that injury-induced activation of STAT3 in the marrow was highly restricted, as there was no clear evidence of differential activation of STAT1, ERK, AKT, p38, or STAT5 pathways in burn injured mice compared to sham injured mice. It was surprising that increased activation of STAT1 or STAT5 in burn injured mice did not occur despite high levels of G-CSF, which has been reported to also act through these signaling intermediates *in vitro* (38).

Recently, STAT3 has been found to play an essential role in G-CSF induced emergency granulopoiesis; regulating proliferation, maturation, and mobilization of neutrophils (39-41). STAT3 is also a signaling intermediate involved in the expansion of myeloid derived suppressor cells (MDSC) (42), a mixed group of immature monocytes, neutrophils and their progenitors that are found in a broad range of inflammatory processes. Our group has previously shown that myeloid cells arising after burn injury are functionally and phenotypically consistent with MDSC, in that they inhibit lymphocyte functions, produce increased levels of reactive oxygen species (ROS) and nitric oxide (NO), and display an altered inflammatory tone with increased ability to produce TNFα and IL-10 (10, 43, 44). Other pathological processes in which MDSC expand include infections, in which MDSC have been found to exhibit antimicrobial activity, and in cancer, where MDSC are thought to suppress tumor killing (45). Tumors have been observed to grow more rapidly in burn injured mice due to defects in cell mediated immune responses (46, 47) and G-CSF driven expansion of granulocytic MDSC has recently been directly implicated in uncontrolled tumor growth (48). Together, these data suggest that myeloid cells that expand after injury due to G-CSF driven STAT3 activation have unique infection fighting properties, and suppress adaptive immune function.

We found that G-CSF was necessary and sufficient for the hematopoietic reprioritization that follows burn injury. Neutralization of G-CSF blocked STAT3 activation, hematopoietic reprioritization and systemic neutrophilia. Exogenous administration of recombinant G-CSF was sufficient to drive myeloid cell expansion in the marrow at the expense of other lineages, similar to burn injury, and protected the animals from a lethal *K. pneumoniae* pulmonary infectious challenge. These data provide strong support that the G-CSF STAT3 axis drives the myeloid shift in the bone marrow and resistance to infection that follows thermal injury.

A similar myeloid shift in the bone marrow occurs in both mice and humans following trauma (24, 25). Our findings in mice and correlative evidence in humans support a prominent role for G-CSF in these hematopoietic changes (49). In the correlative study performed by Cook *et al*. trauma patients with the highest G-CSF levels were found to have greater reductions in hemoglobin and increased transfusion requirements, supporting their conclusion that G-CSF contributes to post-traumatic anemia. Recombinant human G-CSF has previously been shown to suppress bone marrow erythropoiesis in mice although the mechanism of this suppression was not explored (50). Our data indicate that G-CSF is a primary factor produced following injury that reduces the red cell composition of the marrow, although neutralization of G-CSF did not reverse a reduction in red cells we

detected in the blood seven days after burn injury. These data indicate that mechanisms other than deficits in bone marrow erythropoiesis contribute to the low peripheral red blood cell counts observed in our model. Interestingly, Cook et al also reported that trauma patients with the highest GCSF levels had increased rates of infection, shock, acidosis, arterial lactate, or early transfusion requirements (49). Although no attempt to correlate the severity of injury with G-CSF levels or the susceptibility to infection was made in our study, it is reasonable to speculate that there is an optimal G-CSF response and a threshold above which a beneficial response becomes harmful or overwhelmed. In this regard, it is important to note that the incidence of infections, multiple organ failure, and death all increase with burn size (51) and the 15% of total body surface area used in our model may not reflect changes which would be seen following larger burns.

We also found that IL-6 was increased for several days after injury. IL-6 is known to signal through STAT3 and to contribute to emergency granulopoiesis, independent of G-CSF (52). Infection stimulated increases in IL-6 enhance myeloid production and reduce erythroid production in the bone marrow (53). IL-6 and G-CSF have both been reported to arrest B-lymphopoiesis (35, 54) and to cooperatively enhance STAT3 activation in neutrophils (55). Finally, IL-6 may activate hepatic STAT3 and indirectly promote MDSC expansion and recruitment through the upregulation of the acute phase proteins, a mechanism that has been found to play a critical role in surviving sepsis. (56). The acute phase response driven by hepatic STAT3 has also been found to play a critical role in preventing systemic dissemination of infection and mortality following pulmonary infection (57).

Due to the high level of IL-6 that is found in the serum of burn injured mice in our study, and the fact that neutralization of G-CSF did not fully suppress STAT3 activation in bone marrow myeloid and myeloid progenitor cells, we speculate that IL-6 may contribute to the hematopoietic changes and resistance to infection in our model through direct activation of myeloid STAT3 and possibly hepatic STAT3. IL-6 may also contribute to the anemia that follows traumatic injury, as it has been shown to cause hypoferremia in mice and humans by inducing the expression of hepcidin (58). Iron deficiency is a likely mechanism by which erythropoiesis is limited in burn injured humans (59).

We compared the molecular responses of whole blood leukocytes from G-CSF treated humans and trauma patients using datasets from the Gene Expression Omnibus (GEO) repository, and found the molecular responses to be remarkably similar, with both G-CSF and trauma inducing upregulation of innate immunity genes and downregulation of adaptive immunity genes. G-CSF is known to enhance the phagocytic and bactericidal activity of human neutrophils (60). Neutrophils from G-CSF treated humans exhibit increased surface expression of CD11b/CD18 antigen (61) and enhanced oxidative function following stimulation (62), consistent with a heightened state of activation. G-CSF mediated expansion of MDSC may represent one mechanism of suppression of adaptive immune functions following injury, although a substantial body of literature indicates that G-CSF promotes a functionally tolerant adaptive immune response through a variety of mechanisms (63, 64). The functional effects of G-CSF on adaptive immunity include preferential suppression of lymphocyte Th1 responses in association with a shift towards the Th2 phenotype (65-67). Proliferative responses following exposure to mitogens or anti-CD3 are impaired in lymphocytes collected from humans given consecutive doses of G-CSF. Finally, human bone marrow contains large numbers of highly functional CD4+CD25+ T regulatory cells which are mobilized into circulation following consecutive doses of G-CSF and are found to be more potent inhibitors of Th1 cytokine production and lymphocyte proliferation than their counterparts which normally reside in the blood (68). G-CSF mediated mobilization may be relevant to human trauma victims, in that Th1 suppressing CD4+CD25+ T

regulatory cell numbers and activity are increased in the peripheral blood of these patients (22).

The utility of G-CSF for patients suffering from pneumonia and sepsis has been assessed in numerous clinical studies and a benefit has not been proven (69). In our model of injury, the protection against pulmonary infection afforded by G-CSF is time dependent, suggesting that studies designed to assess benefit of prophylactic administration of G-CSF on pneumonia may be more likely to show an effect. Animal models generally support this idea, demonstrating that the pre-emptive use of G-CSF is protective against pneumonia while more inconsistent results are seen when G-CSF is administered following pulmonary infection (70). However, conflicting reports indicate that prophylactic G-CSF may also enhance mortality following pulmonary infection. In one study, a strain of K. *pneumoniae* was able utilize G-CSF to enhance its own capsule production resulting in reduced phagocytic uptake by neutrophils and enhanced mortality (71). Another group reported that G-CSF was protective against *Staphylococcus aureus* pulmonary infection while lung injury and death where enhanced by G-CSF following an *E. coli* challenge, possibly related to a heightened inflammatory response (72). Together these studies suggest the G-CSF response can be both beneficial and harmful and underscore the need for a better understanding of the role of G-CSF in modulating inflammatory tone in patients with severe infection.

In summary, we find that G-CSF plays a central role in post-traumatic resistance to infection and prioritization of bone marrow responses. Although it is widely appreciated that serum G-CSF is increased in traumatized humans, we find it surprising that a single hematopoietic cytokine appears to drive much of the transcriptional signature of injury and function as a node that activates innate immune responses and suppresses adaptive immune responses. Recent reports that the transcriptional response to injury in mice and humans is substantially different (73) notwithstanding, our findings and those of others support a larger role for G-CSF in the response to injury of both species than has formerly been recognized. We submit that G-CSF plays a determinative role in the survival of post injury infection, and that future studies of the post injury G-CSF STAT3 axis are warranted.

Supplementary Material

Refer to Web version on PubMed Central for supplementary material.

References

1. Xiao W, Mindrinos MN, Seok J, Cuschieri J, Cuenca AG, Gao H, Hayden DL, Hennessy L, Moore EE, Minei JP, Bankey PE, Johnson JL, Sperry J, Nathens AB, Billiar TR, West MA, Brownstein BH, Mason PH, Baker HV, Finnerty CC, Jeschke MG, Lopez MC, Klein MB, Gamelli RL, Gibran NS, Arnoldo B, Xu W, Zhang Y, Calvano SE, McDonald-Smith GP, Schoenfeld DA, Storey JD, Cobb JP, Warren HS, Moldawer LL, Herndon DN, Lowry SF, Maier RV, Davis RW, Tompkins RG, Inflammation P, Host Response to Injury Large-Scale Collaborative Research. A genomic storm in critically injured humans. The Journal of experimental medicine. 2011; 208:2581–2590. [PubMed: 22110166]
2. Paterson HM, Murphy TJ, Purcell EJ, Shelley O, Kriynovich SJ, Lien E, Mannick JA, Lederer JA. Injury primes the innate immune system for enhanced Toll-like receptor reactivity. Journal of immunology (Baltimore, Md.: 1950). 2003; 171:1473–1483.
3. Murphy TJ, Paterson HM, Kriynovich S, Zang Y, Kurt-Jones EA, Mannick JA, Lederer JA. Linking the “two-hit” response following injury to enhanced TLR4 reactivity. Journal of leukocyte biology. 2005; 77:16–23. [PubMed: 15496450]
4. Oppeltz RF, Rani M, Zhang Q, Schwacha MG. Burn-induced alterations in toll-like receptor-mediated responses by bronchoalveolar lavage cells. Cytokine. 2011; 55:396–401. [PubMed: 21696980]

5. Maung AA, Fujimi S, Miller ML, MacConmara MP, Mannick JA, Lederer JA. Enhanced TLR4 reactivity following injury is mediated by increased p38 activation. Journal of leukocyte biology. 2005; 78:565–573. [PubMed: 15857937]
6. Kasten KR, Goetzman HS, Reid MR, Rasper AM, Adediran SG, Robinson CT, Cave CM, Solomkin JS, Lentsch AB, Johannigman JA, Caldwell CC. Divergent adaptive and innate immunological responses are observed in humans following blunt trauma. BMC immunology. 2010; 11:4. [PubMed: 20100328]
7. Hietbrink F, Koenderman L, Rijkers G, Leenen L. Trauma: the role of the innate immune system. World journal of emergency surgery : WJES. 2006; 1:15. [PubMed: 16759367]
8. Maung AA, Fujimi S, MacConmara MP, Tajima G, McKenna AM, Delisle AJ, Stallwood C, Onderdonk AB, Mannick JA, Lederer JA. Injury enhances resistance to Escherichia coli infection by boosting innate immune system function. J Immunol. 2008; 180:2450–2458. [PubMed: 18250454]
9. Alexander JW. Effect of thermal injury upon the early resistance to infection. The Journal of surgical research. 1968; 8:128–137. [PubMed: 4966202]
10. Noel G, Wang Q, Osterburg A, Schwemberger S, James L, Haar L, Giacalone N, Thomas I, Ogle C. A ribonucleotide reductase inhibitor reverses burn-induced inflammatory defects. Shock. 2010; 34:535–544. [PubMed: 20386495]
11. Stieritz DD, Holder IA. Experimental studies of the pathogenesis of infections due to Pseudomonas aeruginosa: description of a burned mouse model. The Journal of infectious diseases. 1975; 131:688–691. [PubMed: 805812]
12. Pinto M, Zehavi-Willner T. Thermal injury-induced non-specific resistance to fatal Pseudomonas aeruginosa burn-infection in mice. The Japanese journal of experimental medicine. 1989; 59:189–196. [PubMed: 2559218]
13. Chambler K, Batchelor JR. Influence of defined incompatibilities and area of burn on skin-homograft survival in burned-subjects. Lancet. 1969; 1:16–18. [PubMed: 4178764]
14. Munster AM, Eurenius K, Katz RM, Canales L, Foley FD, Mortensen RF. Cell-mediated immunity after thermal injury. Ann Surg. 1973; 177:139–143. [PubMed: 4144600]
15. Duan X, Yarmush D, Leeder A, Yarmush ML, Mitchell RN. Burn-induced immunosuppression: attenuated T cell signaling independent of IFN-gamma- and nitric oxide-mediated pathways. J Leukoc Biol. 2008; 83:305–313. [PubMed: 18024716]
16. Patenaude J, D'Elia M, Hamelin C, Garrel D, Bernier J. Burn injury induces a change in T cell homeostasis affecting preferentially CD4+ T cells. J Leukoc Biol. 2005; 77:141–150. [PubMed: 15542542]
17. Tschop J, Martignoni A, Reid MD, Adediran SG, Gardner J, Noel GJ, Ogle CK, Neely AN, Caldwell CC. Differential immunological phenotypes are exhibited after scald and flame burns. Shock (Augusta, Ga.). 2009; 31:157–163.
18. Deitch EA, Xu DZ, Qi L. Different lymphocyte compartments respond differently to mitogenic stimulation after thermal injury. Ann Surg. 1990; 211:72–77. [PubMed: 2294848]
19. O'Riordain DS, Mendez MV, Holzheimer RG, Collins K, Mannick JA, Rodrick ML. Interleukin-2 receptor expression and function following thermal injury. Archives of surgery (Chicago, Ill. : 1960). 1995; 130:165–170.
20. Toliver-Kinsky TE, Varma TK, Lin CY, Herndon DN, Sherwood ER. Interferon-gamma production is suppressed in thermally injured mice: decreased production of regulatory cytokines and corresponding receptors. Shock. 2002; 18:322–330. [PubMed: 12392275]
21. O'Sullivan ST, Lederer JA, Horgan AF, Chin DH, Mannick JA, Rodrick ML. Major injury leads to predominance of the T helper-2 lymphocyte phenotype and diminished interleukin-12 production associated with decreased resistance to infection. Ann Surg. 1995; 222:482–490. discussion 490-482. [PubMed: 7574928]
22. MacConmara MP, Maung AA, Fujimi S, McKenna AM, Delisle A, Lapchak PH, Rogers S, Lederer JA, Mannick JA. Increased CD4+ CD25+ T regulatory cell activity in trauma patients depresses protective Th1 immunity. Ann Surg. 2006; 244:514–523. [PubMed: 16998360]

23. MacConmara MP, Tajima G, O'Leary F, Delisle AJ, McKenna AM, Stallwood CG, Mannick JA, Lederer JA. Regulatory T cells suppress antigen-driven CD4 T cell reactivity following injury. J Leukoc Biol. 2011; 89:137–147. [PubMed: 20884652]
24. Livingston DH, Anjaria D, Wu J, Hauser CJ, Chang V, Deitch EA, Rameshwar P. Bone marrow failure following severe injury in humans. Ann Surg. 2003; 238:748–753. [PubMed: 14578739]
25. Posluszny JA Jr. Muthumalaiappan K, Kini AR, Szilagyi A, He LK, Li Y, Gamelli RL, Shankar R. Burn injury dampens erythroid cell production through reprioritizing bone marrow hematopoietic response. J Trauma. 2011; 71:1288–1296. [PubMed: 22071930]
26. Still JM Jr. Belcher K, Law EJ, Thompson W, Jordan M, Lewis M, Saffle J, Hunt J, Purdue GF, Waymack JP, et al. A double-blinded prospective evaluation of recombinant human erythropoietin in acutely burned patients. J Trauma. 1995; 38:233–236. [PubMed: 7869442]
27. Posluszny JA Jr. Conrad P, Halerz M, Shankar R, Gamelli RL. Classifying transfusions related to the anemia of critical illness in burn patients. J Trauma. 2011; 71:26–31. [PubMed: 21131855]
28. Neely AN, Hoover DL, Holder IA, Cross AS. Circulating levels of tumour necrosis factor, interleukin 6 and proteolytic activity in a murine model of burn and infection. Burns. 1996; 22:524–530. [PubMed: 8909752]
29. Domenico P, Diedrich DL, Straus DC. Extracellular polysaccharide production by Klebsiella pneumoniae and its relationship to virulence. Canadian journal of microbiology. 1985; 31:472–478. [PubMed: 3891056]
30. Wei RQ, Yee JB, Straus DC, Hutson JC. Bactericidal activity of testicular macrophages. Biology of reproduction. 1988; 38:830–835. [PubMed: 2840982]
31. Krutzik PO, Clutter MR, Nolan GP. Coordinate analysis of murine immune cell surface markers and intracellular phosphoproteins by flow cytometry. Journal of immunology (Baltimore, Md. : 1950). 2005; 175:2357–2365.
32. Tung JW, Heydari K, Tirouvanziam R, Sahaf B, Parks DR, Herzenberg LA, Herzenberg LA. Modern flow cytometry: a practical approach. Clinics in laboratory medicine. 2007; 27:453–468. v. [PubMed: 17658402]
33. van Eeden SF, Klut ME, Walker BA, Hogg JC. The use of flow cytometry to measure neutrophil function. Journal of immunological methods. 1999; 232:23–43. [PubMed: 10618507]
34. Chakraborty A, Tweardy DJ. Stat3 and G-CSF-induced myeloid differentiation. Leukemia & lymphoma. 1998; 30:433–442. [PubMed: 9711905]
35. Maeda K, Malykhin A, Teague-Weber BN, Sun XH, Farris AD, Coggeshall KM. Interleukin-6 aborts lymphopoiesis and elevates production of myeloid cells in systemic lupus erythematosus-prone B6.Sle1.Yaa animals. Blood. 2009; 113:4534–4540. [PubMed: 19224760]
36. Nicola NA, Begley CG, Metcalf D. Identification of the human analogue of a regulator that induces differentiation in murine leukaemic cells. Nature. 1985; 314:625–628. [PubMed: 2986009]
37. Buzzeo MP, Yang J, Casella G, Reddy V. Hematopoietic stem cell mobilization with G-CSF induces innate inflammation yet suppresses adaptive immune gene expression as revealed by microarray analysis. Experimental hematology. 2007; 35:1456–1465. [PubMed: 17761290]
38. Tian SS, Tapley P, Sincich C, Stein RB, Rosen J, Lamb P. Multiple signaling pathways induced by granulocyte colony-stimulating factor involving activation of JAKs, STAT5, and/or STAT3 are required for regulation of three distinct classes of immediate early genes. Blood. 1996; 88:4435–4444. [PubMed: 8977235]
39. Panopoulos AD, Zhang L, Snow JW, Jones DM, Smith AM, El Kasmi KC, Liu F, Goldsmith MA, Link DC, Murray PJ, Watowich SS. STAT3 governs distinct pathways in emergency granulopoiesis and mature neutrophils. Blood. 2006; 108:3682–3690. [PubMed: 16888100]
40. Zhang H, Nguyen-Jackson H, Panopoulos AD, Li HS, Murray PJ, Watowich SS. STAT3 controls myeloid progenitor growth during emergency granulopoiesis. Blood. 2010; 116:2462–2471. [PubMed: 20581311]
41. Nguyen-Jackson H, Panopoulos AD, Zhang H, Li HS, Watowich SS. STAT3 controls the neutrophil migratory response to CXCR2 ligands by direct activation of G-CSF-induced CXCR2 expression and via modulation of CXCR2 signal transduction. Blood. 2010; 115:3354–3363. [PubMed: 20185584]

42. Gabrilovich DI, Nagaraj S. Myeloid-derived suppressor cells as regulators of the immune system. Nature reviews. Immunology. 2009; 9:162–174.
43. Noel J, G, Osterburn A, Q W, Guo X, D B, Schwemberger S, Goetzman H, Caldwell CC, C O. Thermal Injury elevates the inflammatory monocyte subpopulation in multiple compartments. Shock. 2007
44. Noel G, Wang Q, Schwemberger S, Hanson C, Giacalone N, Haar L, Ogle CK. Neutrophils, not monocyte/macrophages, are the major splenic source of postburn IL-10. Shock. 2011; 36:149–155. [PubMed: 21558983]
45. Cuenca AG, Delano MJ, Kelly-Scumpia KM, Moreno C, Scumpia PO, Laface DM, Heyworth PG, Efron PA, Moldawer LL. A paradoxical role for myeloid-derived suppressor cells in sepsis and trauma. Mol.Med. 2011; 17:281–292. [PubMed: 21085745]
46. Munster AM, Gale GR, Hunt HH. Accelerated tumor growth following experimental burns. J Trauma. 1977; 17:373–375. [PubMed: 859189]
47. Ikeuchi S, Aikawa N, Okuda M, Ishibiki K, Abe O. Changes in cell-mediated immunity and tumour growth after thermal injury. Burns. 1981; 7:400–408.
48. Waight JD, Hu Q, Miller A, Liu S, Abrams SI. Tumor-derived G-CSF facilitates neoplastic growth through a granulocytic myeloid-derived suppressor cell-dependent mechanism. PloS one. 2011; 6:e27690. [PubMed: 22110722]
49. Cook KM, Sifri ZC, Baranski GM, Mohr AM, Livingston DH. The role of plasma granulocyte colony stimulating factor and bone marrow dysfunction after severe trauma. Journal of the American College of Surgeons. 2013; 216:57–64. [PubMed: 23063381]
50. Lord BI, Molineux G, Pojda Z, Souza LM, Mermod JJ, Dexter TM. Myeloid cell kinetics in mice treated with recombinant interleukin-3, granulocyte colony-stimulating factor (CSF), or granulocyte-macrophage CSF in vivo. Blood. 1991; 77:2154–2159. [PubMed: 1709372]
51. Kraft R, Herndon DN, Al-Mousawi AM, Williams FN, Finnerty CC, Jeschke MG. Burn size and survival probability in paediatric patients in modern burn care: a prospective observational cohort study. Lancet. 2012; 379:1013–1021. [PubMed: 22296810]
52. Walker F, Zhang HH, Matthews V, Weinstock J, Nice EC, Ernst M, Rose-John S, Burgess AW. IL6/sIL6R complex contributes to emergency granulopoietic responses in G-CSF-and GM-CSF-deficient mice. Blood. 2008; 111:3978–3985. [PubMed: 18156493]
53. Chou DB, Sworder B, Bouladoux N, Roy CN, Uchida AM, Grigg M, Robey PG, Belkaid Y. Stromal-derived IL-6 alters the balance of myeloerythroid progenitors during Toxoplasma gondii infection. J Leukoc Biol. 2012; 92:123–131. [PubMed: 22493080]
54. Winkler IG, Bendall LJ, Forristal CE, Helwani F, Nowlan B, Barbier V, Shen Y, Cisterne A, Sedger LM, Levesque JP. B-lymphopoiesis is stopped by mobilizing doses of G-CSF and is rescued by overexpression of the anti-apoptotic protein Bcl2. Haematologica. 2013; 98:325–333. [PubMed: 22929978]
55. Yan B, Wei JJ, Yuan Y, Sun R, Li D, Luo J, Liao SJ, Zhou YH, Shu Y, Wang Q, Zhang GM, Feng ZH. IL-6 Cooperates with G-CSF To Induce Protumor Function of Neutrophils in Bone Marrow by Enhancing STAT3 Activation. Journal of immunology (Baltimore, Md. : 1950). 2013; 190:5882–5893.
56. Sander LE, Sackett SD, Dierssen U, Beraza N, Linke RP, Muller M, Blander JM, Tacke F, Trautwein C. Hepatic acute-phase proteins control innate immune responses during infection by promoting myeloid-derived suppressor cell function. The Journal of experimental medicine. 2010; 207:1453–1464. [PubMed: 20530204]
57. Quinton LJ, Blahna MT, Jones MR, Allen E, Ferrari JD, Hilliard KL, Zhang X, Sabharwal V, Algul H, Akira S, Schmid RM, Pelton SI, Spira A, Mizgerd JP. Hepatocyte-specific mutation of both NF-kappaB RelA and STAT3 abrogates the acute phase response in mice. J Clin Invest. 2012; 122:1758–1763. [PubMed: 22466650]
58. Nemeth E, Rivera S, Gabayan V, Keller C, Taudorf S, Pedersen BK, Ganz T. IL-6 mediates hypoferremia of inflammation by inducing the synthesis of the iron regulatory hormone hepcidin. J Clin Invest. 2004; 113:1271–1276. [PubMed: 15124018]
59. Deitch EA, Sittig KM. A serial study of the erythropoietic response to thermal injury. Ann Surg. 1993; 217:293–299. [PubMed: 8452408]

60. Roilides E, Walsh TJ, Pizzo PA, Rubin M. Granulocyte colony-stimulating factor enhances the phagocytic and bactericidal activity of normal and defective human neutrophils. J Infect Dis. 1991; 163:579–583. [PubMed: 1704903]
61. Falanga A, Marchetti M, Evangelista V, Manarini S, Oldani E, Giovanelli S, Galbusera M, Cerletti C, Barbui T. Neutrophil activation and hemostatic changes in healthy donors receiving granulocyte colony-stimulating factor. Blood. 1999; 93:2506–2514. [PubMed: 10194429]
62. Allen RC, Stevens PR, Price TH, Chatta GS, Dale DC. In vivo effects of recombinant human granulocyte colony-stimulating factor on neutrophil oxidative functions in normal human volunteers. J Infect Dis. 1997; 175:1184–1192. [PubMed: 9129083]
63. Rutella S, Zavala F, Danese S, Kared H, Leone G. Granulocyte colony-stimulating factor: a novel mediator of T cell tolerance. Journal of immunology (Baltimore, Md. : 1950). 2005; 175:7085–7091.
64. Franzke A. The role of G-CSF in adaptive immunity. Cytokine & growth factor reviews. 2006; 17:235–244. [PubMed: 16807060]
65. Sloand EM, Kim S, Maciejewski JP, Van Rhee F, Chaudhuri A, Barrett J, Young NS. Pharmacologic doses of granulocyte colony-stimulating factor affect cytokine production by lymphocytes in vitro and in vivo. Blood. 2000; 95:2269–2274. [PubMed: 10733495]
66. Franzke A, Piao W, Lauber J, Gatzlaff P, Konecke C, Hansen W, Schmitt-Thomsen A, Hertenstein B, Buer J, Ganser A. G-CSF as immune regulator in T cells expressing the GCSF receptor: implications for transplantation and autoimmune diseases. Blood. 2003; 102:734–739. [PubMed: 12676791]
67. Pan L, Delmonte J Jr. Jalonen CK, Ferrara JL. Pretreatment of donor mice with granulocyte colony-stimulating factor polarizes donor T lymphocytes toward type-2 cytokine production and reduces severity of experimental graft-versus-host disease. Blood. 1995; 86:4422–4429. [PubMed: 8541530]
68. Zou L, Barnett B, Safah H, Larussa VF, Evdemon-Hogan M, Mottram P, Wei S, David O, Curiel TJ, Zou W. Bone marrow is a reservoir for CD4+CD25+ regulatory T cells that traffic through CXCL12/CXCR4 signals. Cancer Res. 2004; 64:8451–8455. [PubMed: 15548717]
69. Cheng AC, Stephens DP, Currie BJ. Granulocyte-colony stimulating factor (GCSF) as an adjunct to antibiotics in the treatment of pneumonia in adults. The Cochrane database of systematic reviews. 2007:CD004400. [PubMed: 17443546]
70. Marshall JC. The effects of granulocyte colony-stimulating factor in preclinical models of infection and acute inflammation. Shock. 2005; 24(Suppl 1):120–129. [PubMed: 16374383]
71. Held TK, Mielke ME, Chedid M, Unger M, Trautmann M, Huhn D, Cross AS. Granulocyte colony-stimulating factor worsens the outcome of experimental Klebsiella pneumoniae pneumonia through direct interaction with the bacteria. Blood. 1998; 91:2525–2535. [PubMed: 9516154]
72. Karzai W, von Specht BU, Parent C, Haberstroh J, Wollersen K, Natanson C, Banks SM, Eichacker PQ. G-CSF during Escherichia coli versus Staphylococcus aureus pneumonia in rats has fundamentally different and opposite effects. Am J Respir Crit Care Med. 1999; 159:1377–1382. [PubMed: 10228098]
73. Seok J, Warren HS, Cuenca AG, Mindrinos MN, Baker HV, Xu W, Richards DR, McDonald-Smith GP, Gao H, Hennessy L, Finnerty CC, Lopez CM, Honari S, Moore EE, Minei JP, Cuschieri J, Bankey PE, Johnson JL, Sperry J, Nathens AB, Billiar TR, West MA, Jeschke MG, Klein MB, Gamelli RL, Gibran NS, Brownstein BH, Miller-Graziano C, Calvano SE, Mason PH, Cobb JP, Rahme LG, Lowry SF, Maier RV, Moldawer LL, Herndon DN, Davis RW, Xiao W, Tompkins RG. Genomic responses in mouse models poorly mimic human inflammatory diseases. Proc Natl Acad Sci U S A. 2013; 110:3507–3512. [PubMed: 23401516]

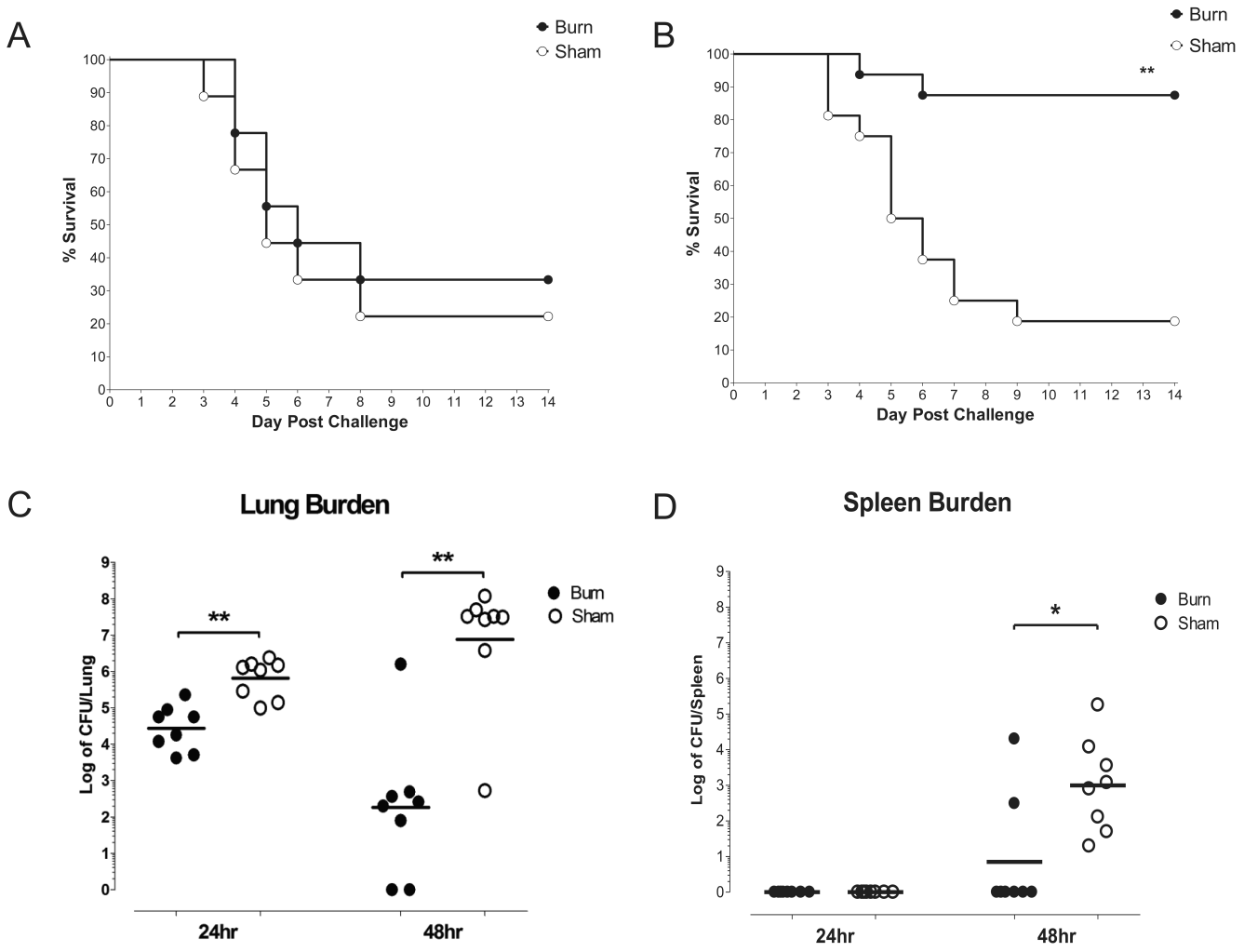

Figure 1. Time dependent survival of burn and sham treated mice after early and late infectious pulmonary challenge

Burn or sham treated mice were infected i.n. with 4×10^4 cfu/mouse *K. pneumoniae* (Panel A) 2 hours or (Panel B) 7 days after thermal injury. Vital status was monitored for 14 days after infection. Kaplan Meier survival curves are shown for infectious challenges delivered 2 hours post injury (n=8 per group) and 7 days post injury (n=16 per group). ** indicates p<.01. Quantitative culture of mice infected at 7 days post injury. (Panel C) Lung and (Panel D) splenic tissues were harvested for quantitative culture at 24 and 48 hours post infection, and microbial burden was quantified as log transformed counts per whole tissue. Line represents the geometric mean of CFUs for n=8 per group. * indicates p<.05, ** indicates p<.01.

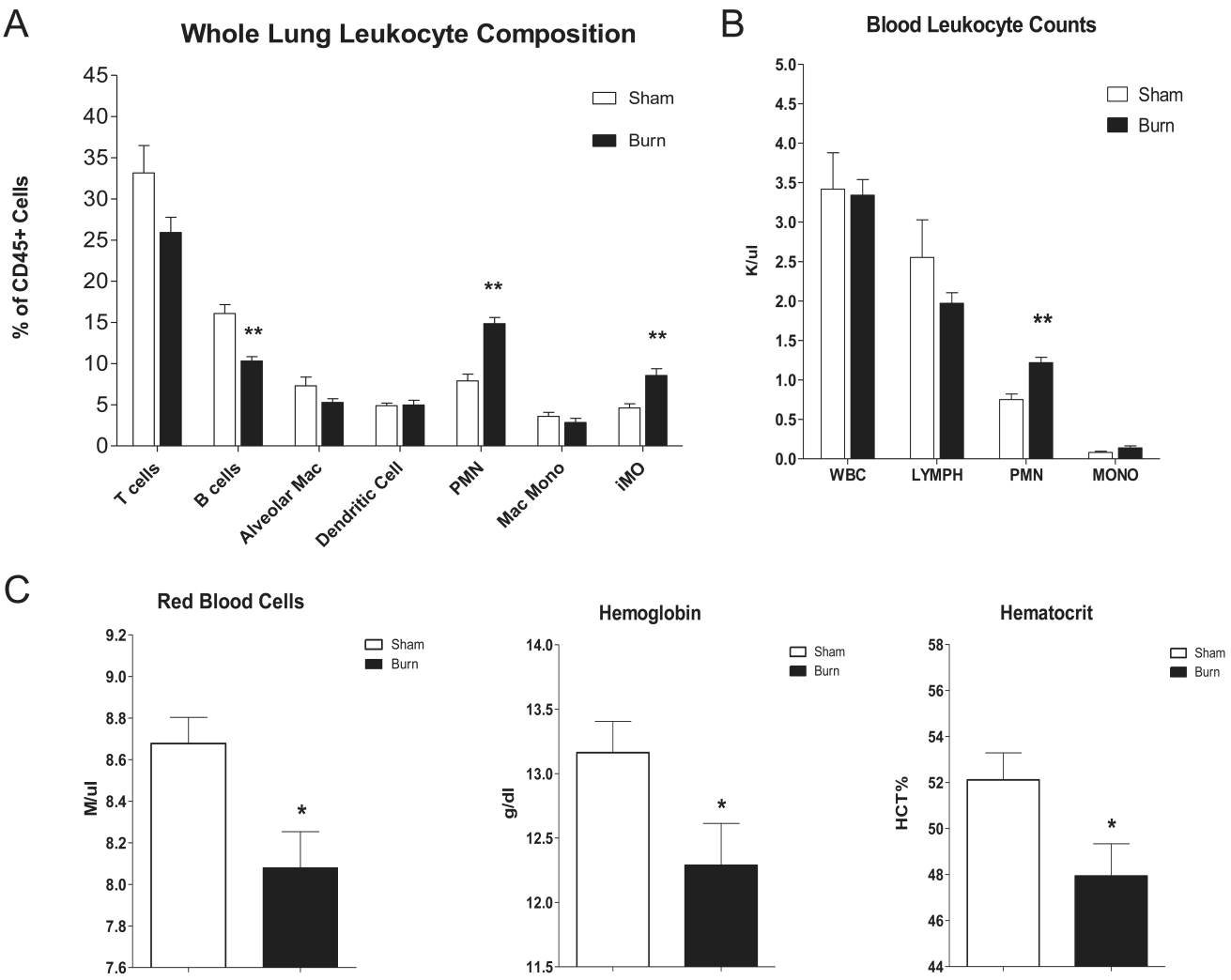

Figure 2. Cellular composition of lung and blood from burn and sham treated mice

Whole lung and blood tissues were harvested 7 days post sham injury or burn treatment. (Panel A) Whole lung leukocyte composition was determined by FACS. (Panel B) Blood leukocyte composition and (Panel C) red cell parameters were determined using an automated cell counter (Hemavet®). Data are expressed as mean values ±SEM for n=8. * indicates $p<.05$ ** indicates $p<.01$

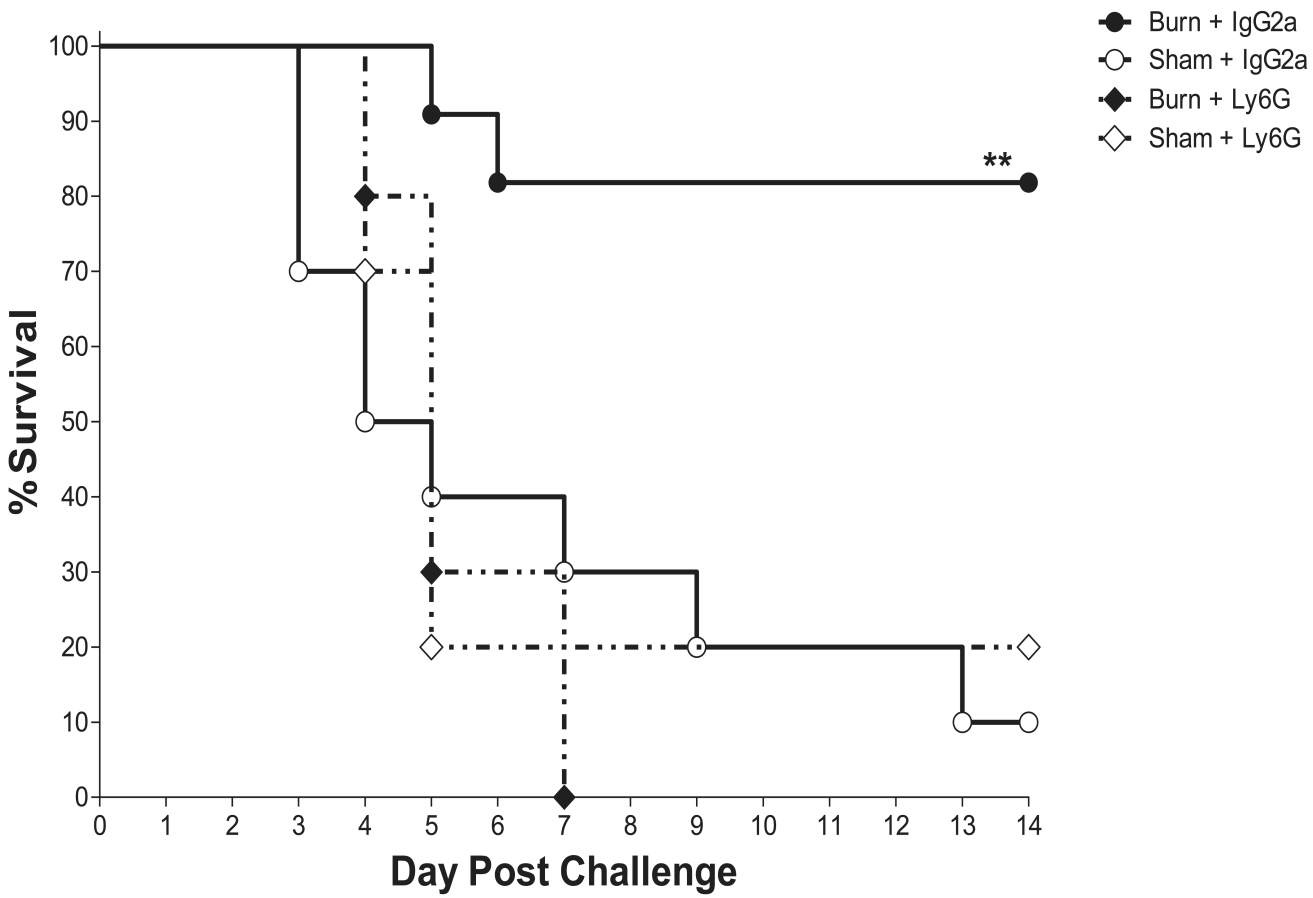

Figure 3. Survival of neutrophil depleted burn and sham treated mice

Neutrophils were quantitatively depleted by administration of anti-Ly6G antibody to burn or sham treated mice as described in methods. Similarly treated control mice were given an IgG2a isotype antibody on the same schedule. All mice were infected i.n. on day 7 post injury with 4×10^4 cfu/mouse *K. pneumoniae*. Vital status was followed for 14 days after infection. Kaplan Meier survival curves are shown for n=10 per group. ** indicates p<.01.

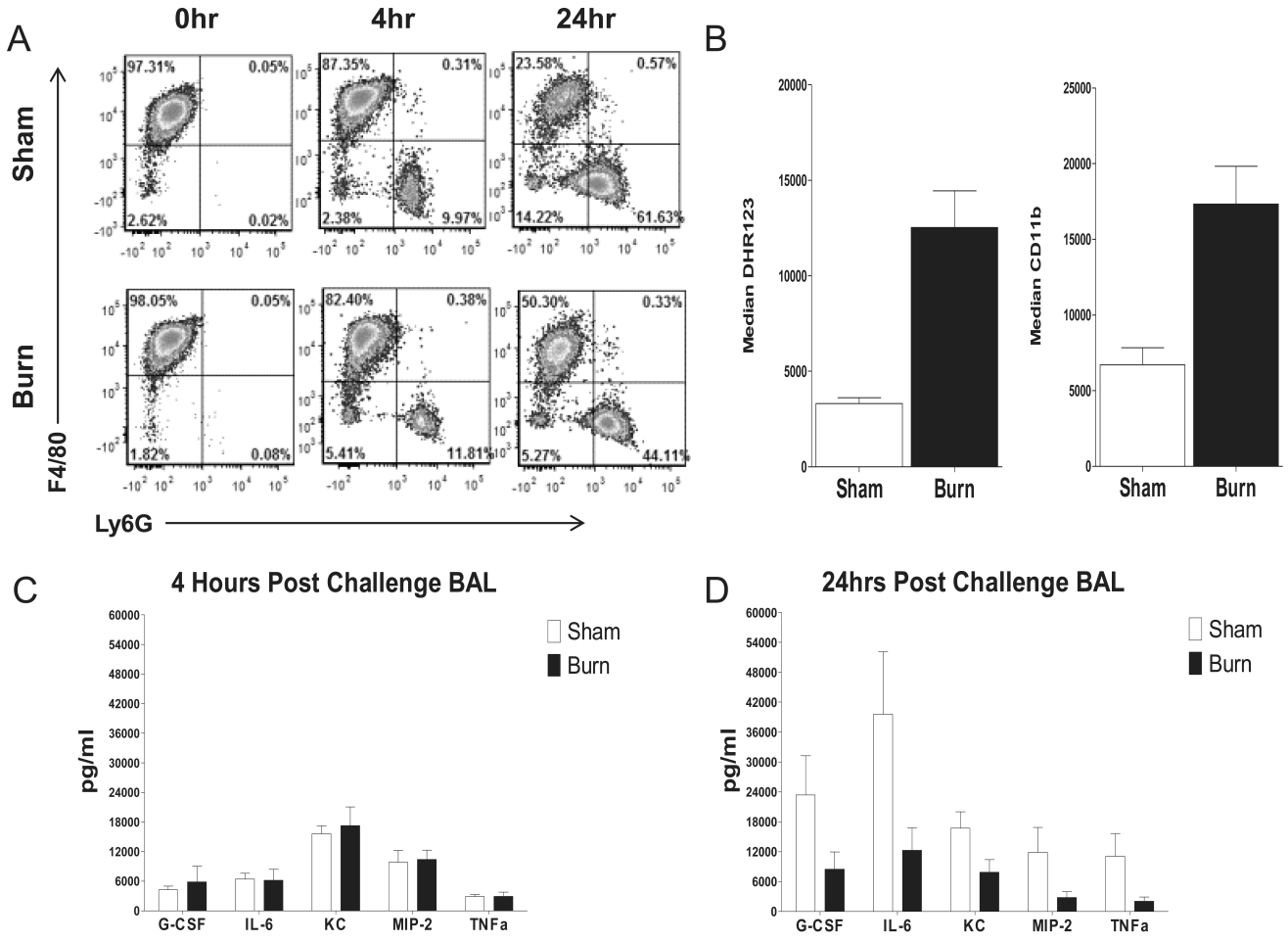

Figure 4. Post infection BAL neutrophil recruitment, function, and airspace inflammatory tone in burn and sham treated mice

7 days post burn or sham treated mice were infected i.n. with 4×10^4 cfu/mouse *K. pneumoniae*. (Panel A) FACS was used to measure the influx of neutrophils (Ly6G+, F4/80− cells) into the airspace at 0, 4 and 24 hours post infection. (Panel B) The PMA stimulated oxidative burst and degranulation response as measured by stimulated increase in CD11b surface expression of BAL neutrophils isolated 4 hours post infection was assessed. Cytokine levels in BAL fluid were determined at (Panel C) 4 hours post infection and (Panel D) 24 hours post infection. Data are expressed as mean values ±SEM for n=4-5 per group. * indicates p<.05 and ** indicates p<.01.

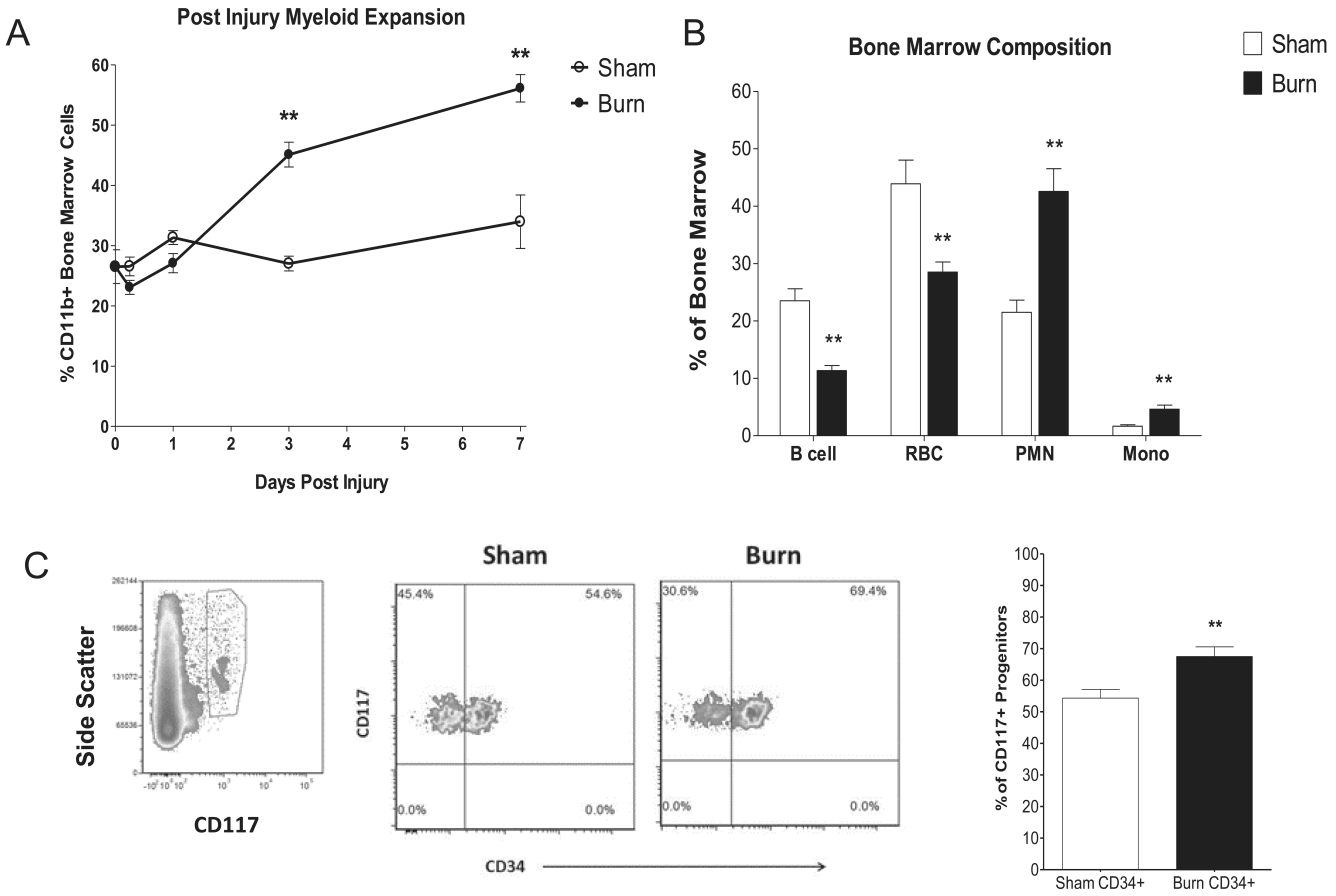

Figure 5. Bone marrow reprioritization in mice exposed to thermal injury

Bone marrow of burn and sham treated mice was isolated from 0-7 days post injury. FACS analysis was used to quantify (Panel A) the percentage of bone marrow cells represented by myeloid lineages (CD11b+) over one week post injury (Panel B), the cellular composition of bone marrow at day 7 post injury, and (Panel C) representative samples depicting gating strategy followed by plot of the proportion of CD117+ progenitors that are CD34+ myeloid progenitor cells at day 7 post injury. Data are expressed as mean values ±SEM for n=4-8 per group. ** indicates p<.01.

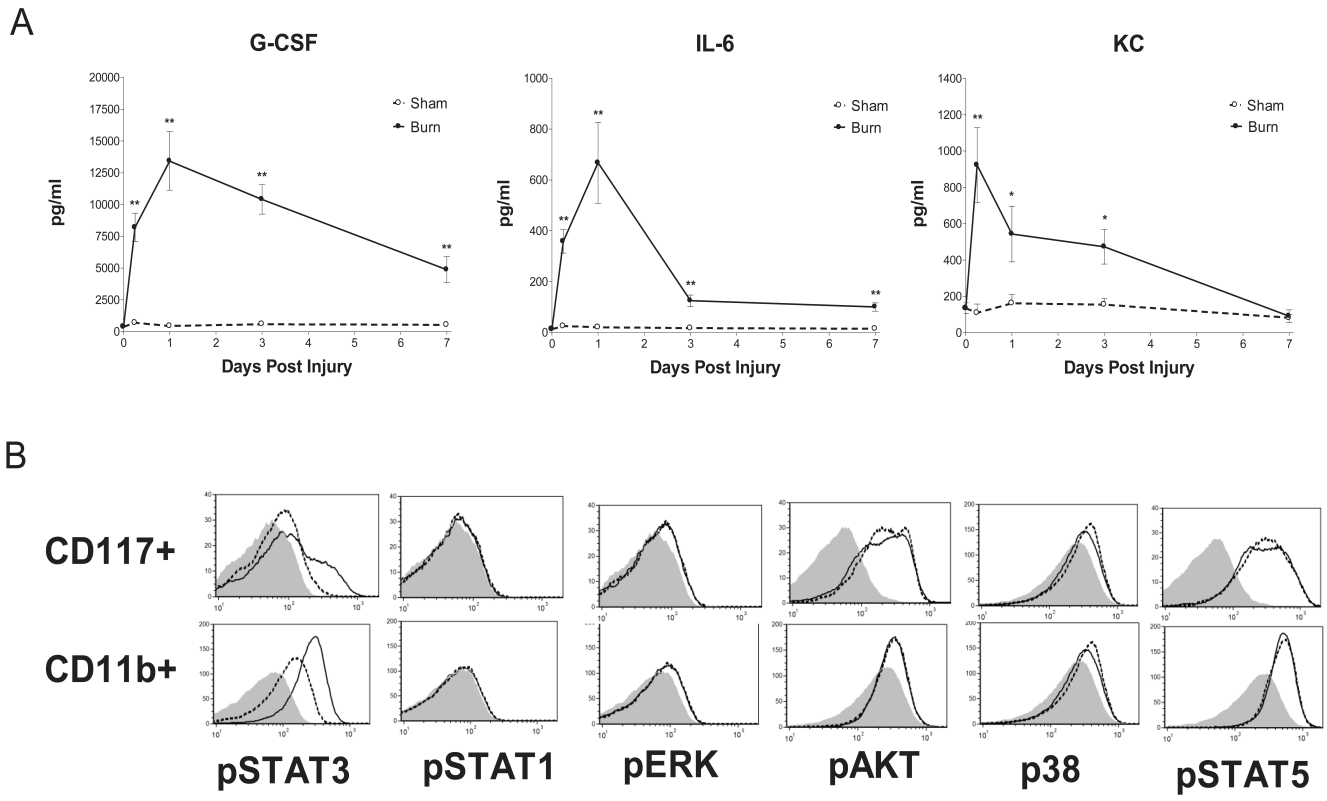

Figure 6. Post injury serum cytokine profile and bone marrow signaling

(Panel A) Serum cytokine concentrations were determined at 0.25, 1, 3, and 7 days post burn or sham. (Panel B) 24 hour post burn vs. sham screen for phosphorylation of key proteins representing nodes in major intracellular signaling pathways in bone marrow CD117+ progenitors and CD11b+ mature myeloid cells. Representative results are shown from bone marrow of a representative burned mouse (solid line), and a representative sham treated mouse (segmented line). Background fluorescence of pooled cells is shown as a shaded area. Cytokine data are expressed as mean values ±SEM for n=4-5 per time point. * indicates p<.05 and ** indicates p<.01.

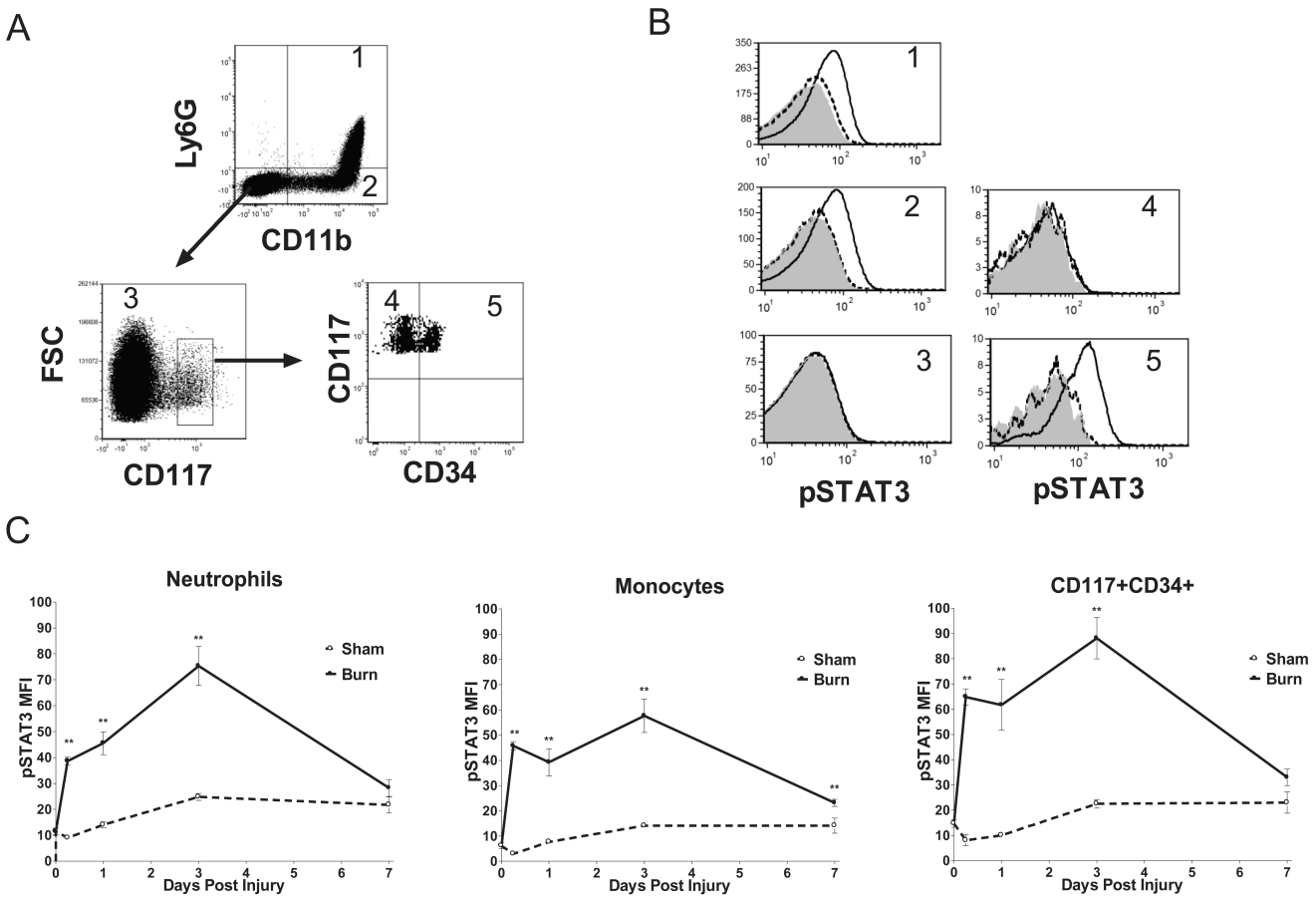

Figure 7. Cell specific STAT3 activation in bone marrow cells of burn and sham treated mice

Bone marrow cells were isolated from burn and sham treated mice 7 days after injury and analyzed by FACS (A) The gating strategy is depicted by arrows and numbers indicate cell type; 1=neutrophils, 2=monocytes, 3=non-myeloid, 4=megakaryocyte erythrocyte progenitors, 5=myeloid progenitors. (Panel B) Representative 24 hour population specific STAT3 activation in burn (solid line), and sham (segmented line) mice, and pooled population background (shaded area). (Panel C) Time course of STAT3 activation in neutrophils, monocytes and myeloid precursors 0.25, 1, 3, and 7 days post burn or sham. Data are expressed as mean values ±SEM for n=4-6 per time point. ** indicates p<.01.

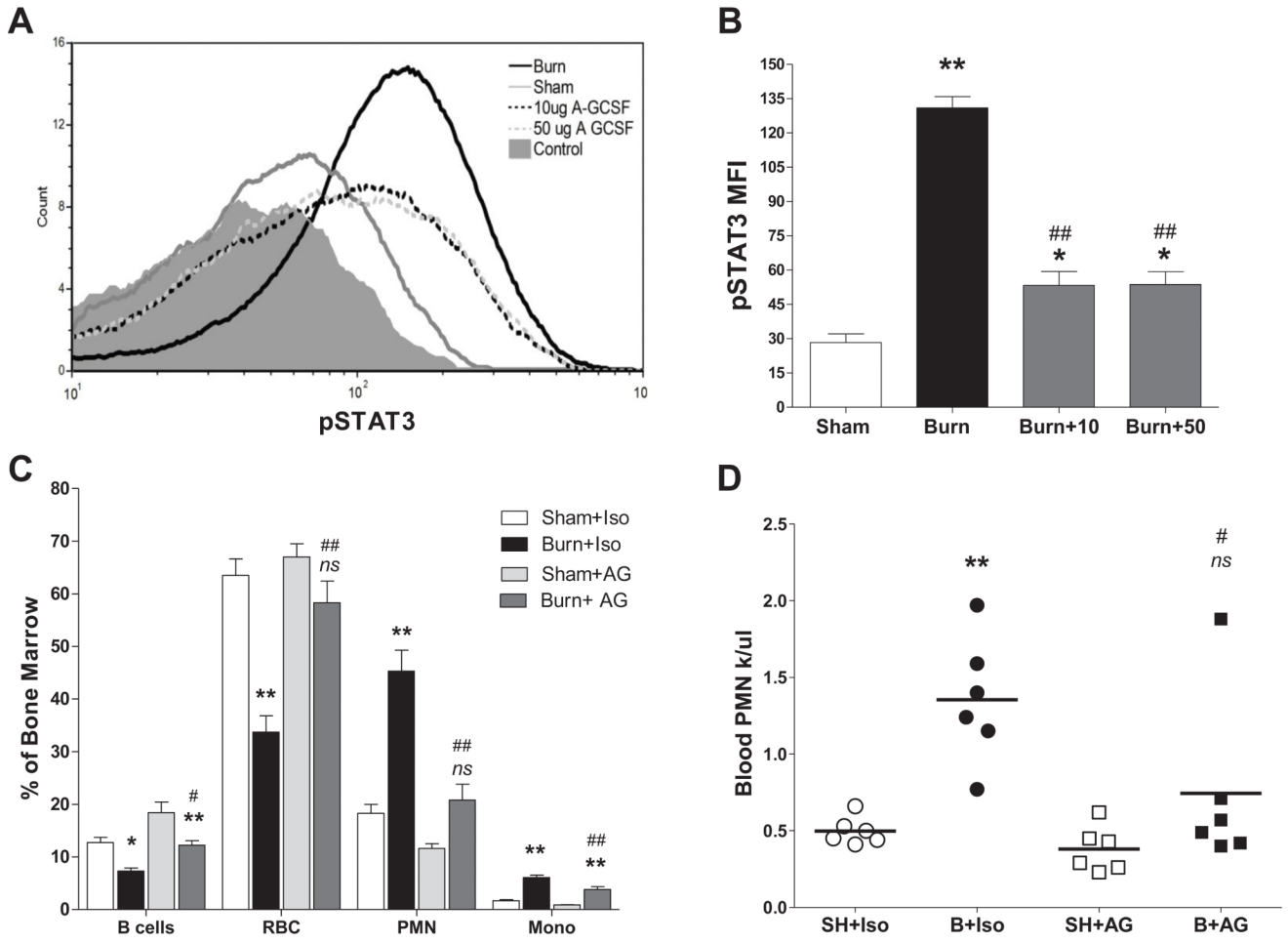

Figure 8. Post burn neutralization of serum G-CSF prevents STAT3 activation, bone marrow reprioritization, and neutrophilia

Mice were given a G-CSF neutralizing antibody. (Panel A) Representative histograms of pSTAT3 in bone marrow CD117+CD34+ bone marrow progenitors 6 hours following sham injury (grey line), burn injury (black line), burn injury + 10μg anti-G-CSF (segmented black line), burn injury + 50μg anti-G-CSF (segmented gray line) and background control staining (shaded area). Anti-G-CSF was delivered i.p. 12 hrs prior to injury and at time of injury. (Panel B) Comparative effects of 10 and 50 μg doses of G-CSF neutralizing antibody on 6 hour post injury pSTAT3. (Panel C) Bone marrow composition 7 days post sham or burn injury in mice treated with daily 10μg doses of anti-G-CSF (AG) or isotype (Iso) antibody as described in methods. (Panel D) Peripheral blood neutrophil counts at 7 days post injury determined in sham isotype (SH+Iso), burn isotype (B+Iso), sham anti-G-CSF (SH+AG), burn anti-G-CSF (B+AG) treated mice. Data represent mean values ±SEM for n=3/group in panel B and n=6/group for panels C and D. Significance determined by ANOVA comparing selected pairs of groups. *Indicates significance burn vs. sham, # indicates significance burn vs. burn, *ns* indicates not significant burn vs. sham. Single indicators $p<.05$ and double indicators $p<.01$.

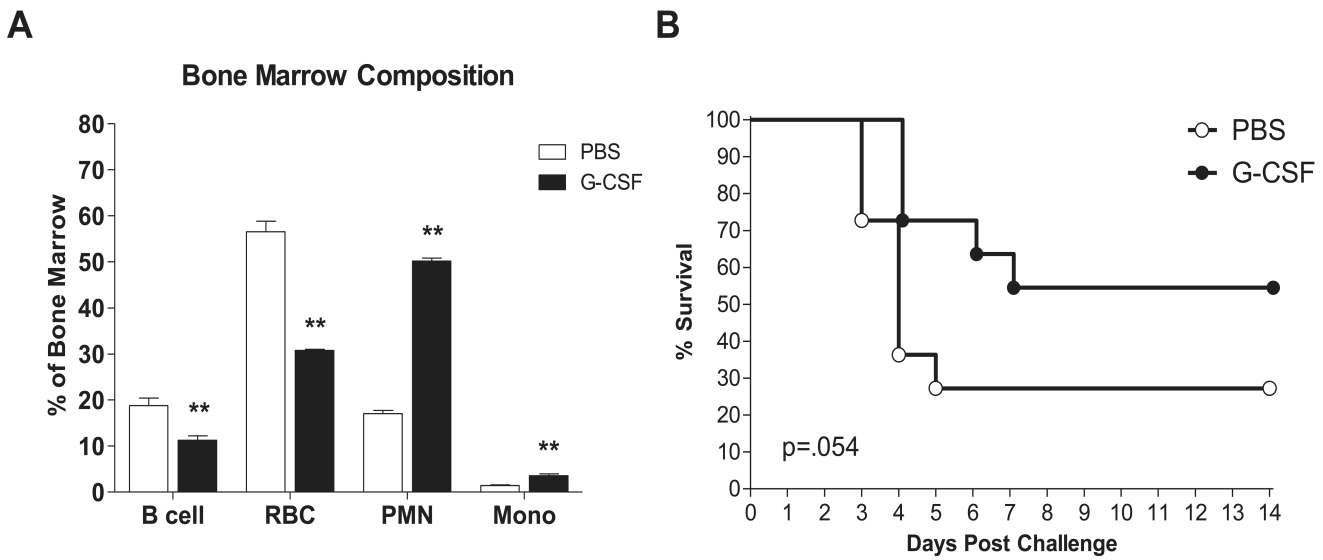

Figure 9. Recombinant G-CSF recapitulates post injury reprioritization and protection from infection

Mice were treated with recombinant mouse G-CSF or PBS as described in methods for six consecutive days prior to bone marrow analysis or infection on day 7. (Panel A) Bone marrow composition was determined by FACS analysis of n=4/group. ** indicates p<.01. (Panel B) Mortality of G-CSF vs. PBS treated mice infected i.n. with 4×10^4 cfu/mouse *K. pneumoniae*. Kaplan Meier survival curves are shown for n=11/group. p=.054.

A

Significant Genes		G-CSF	
		Up	Down
Trauma	Up	**1385**	228
	Down	35	**1673**

B

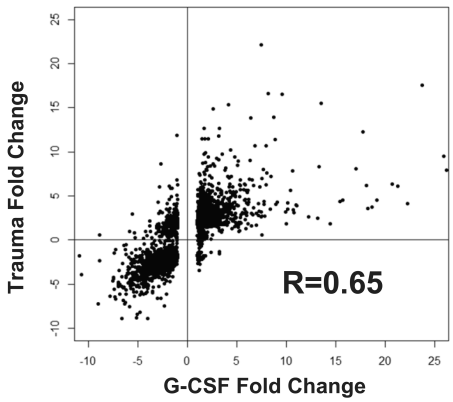

C

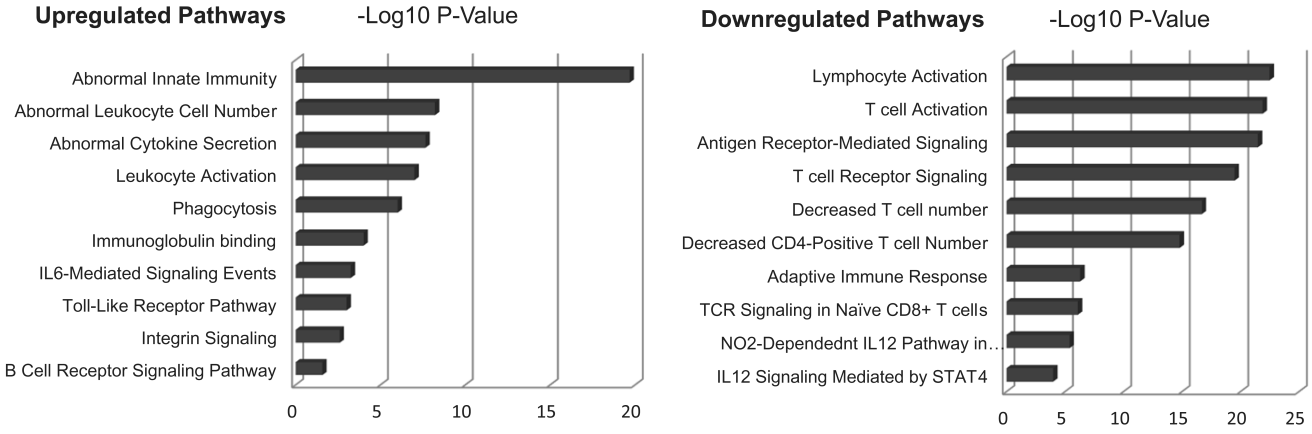

Figure 10. Comparison of the whole blood leukocyte transcriptional response to G-CSF treatment and trauma in humans

A comparison of the whole blood leukocyte transcriptional response in G-CSF treated humans and trauma patients was conducted using publicly available data from the Gene Expression Omnibus (GEO) repository. Genes that exhibited a fold change of ≥2 in response to trauma or G-CSF compared to their respective controls were included in a list of significant genes. (Panel A) Comparison of directional change of genes that were significantly changed following GCSF administration or trauma. (Panel B) Correlation analysis of fold changes following trauma and G-CSF using genes with at least 2 fold change following trauma. (Panel C) Gene ontology enrichment analysis shows pathways most affected by G-CSF and Trauma.